Atmospheric Environment 205 (2019) 36–45

Contents lists available at ScienceDirect

Atmospheric Environment

journal homepage: www.elsevier.com/locate/atmosenv

Characterization of $PM_{2.5}$ source profiles from typical biomass burning of maize straw, wheat straw, wood branch, and their processed products (briquette and charcoal) in China

Jian Sun[a,c], Zhenxing Shen[b,*], Yue Zhang[b], Qian Zhang[b], Yali Lei[b], Yu Huang[c], Xinyi Niu[d], Hongmei Xu[b], Junji Cao[c], Steven Sai Hang Ho[e], Xuxiang Li[a]

[a] School of Human Settlements and Civil Engineering, Xi'an Jiaotong University, Xi'an, 710049, China
[b] Department of Environmental Science and Engineering, Xi'an Jiaotong University, Xi'an, 710049, China
[c] Key Lab of Aerosol Chemistry & Physics, SKLLQG, Institute of Earth Environment, Chinese Academy of Sciences, Xi'an, 710049, China
[d] The Jockey Club School of Public Health and Primary Care, The Chinese University of Hong Kong, Hong Kong, China
[e] Divison of Atmospheric Sciences, Desert Research Institute, Reno, NV89512, United States

GRAPHICAL ABSTRACT

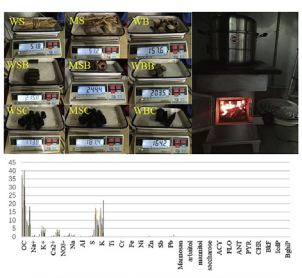

ARTICLE INFO

Keywords:
Source profiles
Biomass burning
Briquette
Charcoal
Fuel processing

ABSTRACT

Chemical profiles from burning of raw biomass materials (i.e., maize straw, wheat straw and wood branch) and their processed products (i.e., briquette and charcoal) were determined with a customized cleaning stove in a combustion chamber. Inorganic species such as water-soluble ions and elements, and carbonaceous fractions including saccharide and polycyclic aromatic hydrocarbons (PAHs) in fine particulate matter ($PM_{2.5}$) were quantified. Organic carbon (OC) was the highest fraction with a mass contribution to $PM_{2.5}$ ranging from 17.65 ± 0.15% to 40.17 ± 3.83%. Potassium (K^+) and chloride (Cl^-) were the two most abundant water-soluble ions (4.31 ± 1.57% and 3.05 ± 1.29%, respectively). Most elements (e.g., heavy metals) had relatively low fractions (< 0.01%) or below detection limit. For organics, levoglucosan averagely accounted for over 60% in total quantified saccharides, while 4-ring PAHs was the most dominant fraction. The proportions of OC, sum of quantified PAHs (ΣPAHs) and levoglucosan, as well as diagnostic ratios such as OC/element carbon (EC), K^+/EC, and sum of quantified saccharides (Σsaccharides)/$PM_{2.5}$ showed a characteristic descending order of raw fuels > briquette > charcoal. In comparison, charcoal burning had lower fractions of the organics since most volatile matters and moisture had been removed during carbonization. In addition, the similarities of chemical profiles from different bio-fuels burning were assessed by calculating the coefficient of divergence (CD) and their correlations. Relatively low CD (0.21–0.36) and high correlation (R > 0.97) suggest that the chemical profiles from straw and their briquettes were similar. However, the profiles from charcoal burning showed significant differences between their corresponding raw fuels (CDs = 0.26–0.47, R = 0.69–0.99) and also large variations

* Corresponding author.
E-mail address: zxshen@mail.xjtu.edu.cn (Z. Shen).

https://doi.org/10.1016/j.atmosenv.2019.02.038
Received 14 October 2018; Received in revised form 19 January 2019; Accepted 24 February 2019
Available online 02 March 2019
1352-2310/

from each other (CDs = 0.40–0.49, $R < 0.90$). The results of this study summarize that the processed fuels especially charcoals are unique in source apportionment and inventory studies.

1. Introduction

Biomass burning either for residential usage or from natural occurrence has been widely concerned in China due to its massive emissions of air pollutants to the environment (Shen et al., 2009, 2015; Ni et al., 2015; Niu et al., 2017; Tao et al., 2015). In order to measure the contribution of biomass burning to ambient fine particulate matter ($PM_{2.5}$), different chemical characterization methods and receptor models have been applied (Mo et al., 2016). It is therefore critical to obtain their source profiles, expressed as the weight fraction of each component relative to the total emission mass, for building up a full chemical emission inventories (Watson et al., 2001).

The $PM_{2.5}$ source profiles on biomass burning have been obtained in many studies (Sheesley et al., 2007; Turn et al., 1997; Watson et al., 2001). Ni et al. (2017) summarized the $PM_{2.5}$ source profiles for open burning of several crop straws in China. Shen et al. (2013) and Zhang et al. (2018) have determined the source profiles for typical woody fuels in field and laboratory-controlled environment, respectively. In recent years, biomass fuels have been being modified by physical and chemical measures due to the environmental concerns. Briquetting and carbonization are the two most popular technologies (Zeng et al., 2007), which would alter the density, moisture, carbon content and many other aspects of the raw materials. Briquette and charcoal are the two representatives of processed fuels which exhibit different $PM_{2.5}$ emission source profiles from their original forms (Ravichandran and Corscadden, 2014; Shen et al., 2013).

Many researches on acquisition of $PM_{2.5}$ emission profiles for different biomass fuels burning have been conducted in China (Ni et al., 2017; Ravichandran and Corscadden, 2014; Shen et al., 2012; Kong et al., 2013). Ni et al. (2017) collected the $PM_{2.5}$ samples from straw open burning and obtained the chemical profiles of carbonaceous fractions, water-soluble ions and elements. Zhang et al. (2013) investigated the carbonaceous profiles of $PM_{2.5}$ for biomass burning. Xu et al. (2006) summarized the $PM_{2.5}$ PAH profiles from typical biomass burning. However, those studies mainly focused on basic components such as carbonaceous fractions, inorganic ions and elements (Ni et al., 2017; Watson et al., 2001; Zhang et al., 2018). Comprehensive organic profiles are rare to be obtained even though many organic compounds have great impacts on the environment and human health. Atmospheric polycyclic aromatic hydrocarbons (PAHs) in China have been found to be mainly contributed from biomass burning (> 60%) (Li et al., 2007a; Tao et al., 2011; Kong et al., 2010). Additionally, biomass burning can emit high abundances of saccharides such as levoglucosan and mannosan (Li et al., 2016; Simoneit et al., 1999). The determination of these organic tracers for different sources is thus critical for characterization of ambient samples using receptor models (e.g., chemical mass balance, CMB) (Robinson et al., 2006; Sheesley et al., 2007).

To obtain systematic source profiles, typical biomass fuels were examined in our laboratory simulated study. Wheat and maize straws were selected because they are the two most common crops, which accounted for > 50% of total straw production in China (Chen et al., 2017). Besides, wood branches were rich in certain areas such as forests and fruit tree economic zones. Apple tree branch was thus selected as it has the largest production in non-forest areas in Northern China, e.g. Guanzhong Plain (Sun et al., 2018b; Zhang et al., 2018). The simulated experiment has advantages to achieve more steady and controllable combustion processes than field measurement. The objectives of this study are: 1) to obtain a comprehensive source profiles for the most common types of biomass fuels burning in China; and 2) to demonstrate the influences of fuel processes on the chemical emissions.

2. Methodology

2.1. Bio-fuel samples

Information of the biomass fuels examined in this study was listed in Table S1 (Supplementary Material). Briefly, raw fuels of maize straw (MS), wheat straw (WS) and wood branch (WB) were collected in nature directly, and others were processed to form briquette and charcoal. The raw and processed fuels were all stored at ambient temperature (~20 °C) and relative humidity (RH, 35–45%) for at least one month before the experiments.

2.2. Sample collection

The combustion experiments were conducted in the Institute of Earth Environment, Chinese Academy of Science, Xi'an, China. Each examined fuel was weighed (50–100 g for each test) and subsequently burnt in a clean stove inside an all-enclosed stainless-steel made environmental combustion chamber (1.8 in length × 1.8 in width × 2.2 m height), which had a total volume of ~8 m^3 (Fig. S1). The combustion conditions and method were well described in our previous publication (Sun et al., 2018b). The smoke emitted from laboratory-simulated stove burning was directed to a dilution sampler at a dilution rate of 5–15 (Tian et al., 2015). A total of nine sets of experiments was obtained, and each was repeated for at least three times. More details on the chamber experiments were reported in Tian et al. (2015) and Sun et al. (2018a).

The $PM_{2.5}$ samples were collected from three parallel channels located downstream of the residence chamber in the dilution sampler at a flow rate of 5 L min^{-1}. Two channels equipped a 47 mm quartz filters (Whatman, Maidstone, UK) and another one equipped with a 47 mm Teflon filter (Pall Life Sciences, Ann Arbor, MI, USA). The Teflon filter was weighed on a microbalance (± 1 mg precision, Sartorius AG MC5, Germany) to obtain the $PM_{2.5}$ mass. The mass concentration of each sample filter was reported by subtracting from the field blank to eliminate any passive gas adsorption artifacts.

2.3. Chemical analysis

2.3.1. OC and EC analysis

Organic carbon (OC) and element carbon (EC) were quantified on a punch (0.526 cm^2) from the quartz-fiber filter by thermal optical reflectance (TOR) technique using a thermal/optical carbon analyzer (DRI Model, 2001; Atmoslytic Inc., Calabasas, CA, USA) with the IMPROVE_A protocol (Chow et al., 2007). The EC and OC concentrations in the sample sets were all above the detection limit (0.01 and 0.39 μg cm^{-2}, respectively).

2.3.2. Water-soluble inorganic ions analysis

One quarter of the quartz-fiber filter was extracted with deionized water (10 mL). The extractants were filtered by microporous membranes (0.45-μm pore size) to remove any insoluble materials. Eight inorganic ions were analyzed with a Dionex ion chromatography (IC) (DX-500, Sunnyvale, CA, USA). The detection limits of Na^+, NH_4^+, K^+, Mg^{2+}, Ca^{2+}, Cl^-, NO_3^-, and SO_4^{2-}, were 4.6, 4.0, 10.0, 4.0, 5.0, 20.0, 15.0 and 0.5 ppb, respectively. Details of the chemical analysis procedures were shown in Shen et al. (2011b).

2.3.3. Element analysis

Energy dispersive X-Ray fluorescence (ED-XRF) spectrometry

(Epsilon 5 ED-XRF, PANalytical B. V., the Netherlands) was used to quantify the elements in $PM_{2.5}$ collected on the Teflon filters (Zhang et al., 2014b). A three-dimensional polarizing geometry contained eleven secondary targets (i.e., CeO_2, CsI, Ag, Mo, Zr, KBr, Ge, Zn, Fe, Ti, and Al) and a barkla target (Al_2O_3), together with good signal to background ratio was accomplished in the analysis. The ED-XRF spectrometer was calibrated with thin-film standards (MicroMatter Co., Arlington, WA, USA). A total of 21 elements were quantified in the analysis.

2.3.4. PAHs and saccharides analysis

One-half of each quartz-fiber filter was extracted with high-purity dichloromethane and methanol (2:1, v/v) under ultrasonication for 15 min. The procedure was repeated three times to ensure the completeness of extraction. Water and debris in the combined extracts were then removed by passing through Pasteur pipettes filled with sodium sulfate (Na_2SO_4) and glass wool. The extracts were finally concentrated to 1 mL by a rotary evaporator under vacuum. Aliquots of the extracts were then reacted with *N,O*-bis-(trimethylsilyl)trifluoroacetamide (BSTFA) containing 1% trimethylchlorosilane and pyridine at 70 °C for 3 h. The functional groups of -COOH and -OH were derivatized to the corresponding trimethylsilyl (TMS) esters and ethers, respectively. One microliter of the reactant was injected into a gas chromatography/mass spectrometer (GC/MS) (Model 7890A/5975C, Agilent Technologies, Santa Clara, CA, USA). More detailed information on the pre-treatment and instrumental settings were shown in Medeiros et al. (2006) and Bi et al. (2008). A total of 16 preferential PAHs and eight saccharides were quantified.

2.4. Statistical analysis

The coefficient of divergence (CD) was applied to testify the similarity of composition profiles and was calculated using Eq. (1):

$$CD_{jk} = \sqrt{\frac{1}{p}\sum_{i=1}^{p}\left(\frac{x_{ij} - x_{ik}}{x_{ij} + x_{ik}}\right)^2} \quad (1)$$

where x_{ij} represents the average concentration of *i*th chemical component at site *j*, *j* and *k* represent two sampling sites, and *p* is the number of measured chemical species (Han et al., 2010). In comparisons between multiple values, one-way analysis of variance (ANOVA) with Tukey's post-hoc test was used for the analysis. The statistical analyses were conducted using GraphPad Prism software (Version 5 for Windows). The significance level was set at $p < 0.05$.

2.5. QA/QC

For each chamber test, at least three replicate samples were obtained to minimize experimental errors. The combustion chamber was cleaned after each test and the inner surface was coated by polytetrafluoroethylene to prevent the reactions and absorption of particles or gaseous pollutants. Before sample collection, all Teflon-membrane filter were pre-conditioned at 25 ± 0.5 °C temperature and 35 ± 5% relative humidity (RH) for 48 h. The quartz microfiber filters were preheated at 900 °C for 3 h before sampling to remove any residual carbon. Experimental blank filters were also collected to correct any passive gas adsorption artifacts.

For chemical analysis, randomly one in ten samples was re-analyzed for quality control and the difference should be < 10% between two replicates (Cao et al., 2007). All chemical analyses were complied with their protocols or standard operation procedures. The analytical instruments were calibrated regularly under the instructions recommended by the manufacturers. The EC and OC concentrations were all above detection limit (1.0 μg m^{-3}) of the instrument. The detection limits of Na^+, NH_4^+, K^+, SO_4^{2-}, NO_3^-, and Cl^- were 4.6, 4.0, 10.0, 0.5, 15.0 and 20.0 μg m^{-3}, respectively. The detection limit for elements and organics were listed in Tables S2 and S3, respectively.

3. Results & discussion

3.1. Carbonaceous, ionic and elemental profiles

The $PM_{2.5}$ mass of each sample collected from the biomass fuels burning was reconstructed by counting the sum of organic matter (OM), EC, inorganic ions, geological minerals, and other elements by different means of chemical analyses (Chow et al., 2015; Wang et al., 2015). The mass reconstruction method was described in S1 (Supplementary Material) and the results were plotted in Fig. 1. The reconstructed masses were equivalent to 88 ± 15% (68–105%) of the gravimetric $PM_{2.5}$ masses, representing that the proposed chemical analyses sufficiently

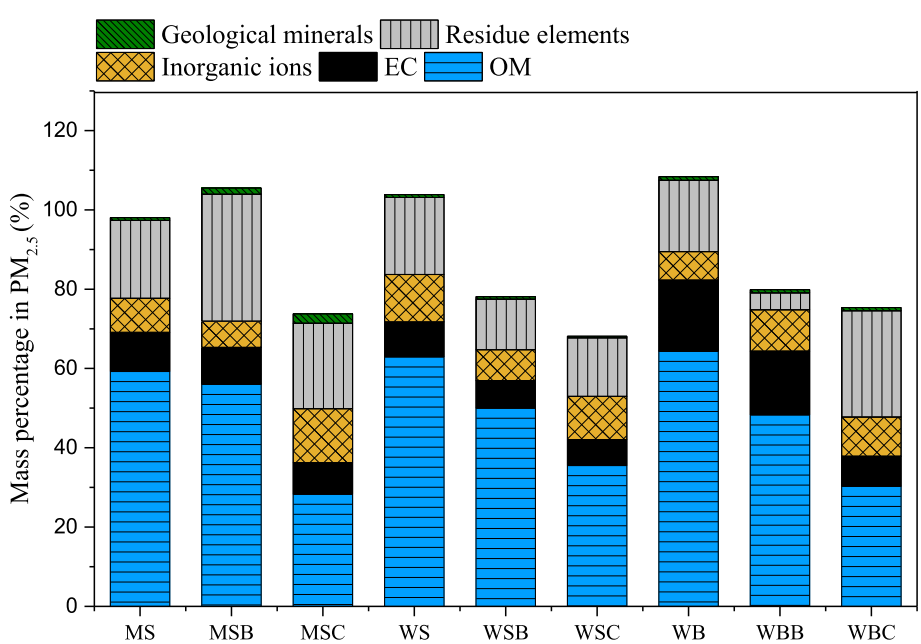

Fig. 1. Mass fractions of major components to $PM_{2.5}$ mass for each biomass fuel burning. Methods to estimate each component were present in Section S1 (supplementary material), and the abbreviation of each fuel refers to Table S1.

covered comprehensive species (Chow et al., 2015; Ni et al., 2017). OM was the most dominant fraction with an average of > 48% (28–64%) of the reconstructed mass, followed by the elements of 18 ± 8% (5–32%). The fractions of the water-soluble ions and EC were both ~10%. However, the values for the water-soluble ions were relatively more consistent in the samples. The geological minerals showed the lowest contribution to the reconstructed mass (< 1%). This feature is useful to identify the contribution of biomass burning from other pollution sources such as urban dust (Shen et al., 2016; Sun et al., 2019; Zhang et al., 2014a).

Table 1 shows the chemical profile for each bio-fuel burning. OC was the most abundant component, ranging from 17.7 to 40.2% to $PM_{2.5}$ mass. EC ranged from 1.47 to 18.4%, being the second contributor. It should be noted that there was no significant difference on the OC contributions among the three raw straws [i.e., maize straw (MS), wheat straw (WS) and wood branch (WB)]. However, in comparison, the burning of processed fuels of briquette [i.e., maize straw briquette (MSB), wheat straw briquette (WSB) and wood branch briquette (WBB)] and charcoal [i.e., maize straw charcoal (MSC), wheat straw charcoal (WSC) and wood branch charcoal (WBC)] showed much lower fractions of both OC and EC. The OC for charcoal burning were 54%, 44% and 55%, respectively, lower than those of MS, WS and WB. Similar phenomenon was observed for EC. On one side, the higher density of briquettes and charcoal compared with the raw fuels reduces the burning rates and consequently suppresses the productions of incomplete combustion products (Shen et al., 2015; Sun et al., 2018b). On another side, the carbonization processes could remove most volatile matters in the biomass fuels (Zeng et al., 2007) (Table S1), minimizing the OC and EC generations during the combustion (Liu et al., 2001). It could be thus concluded that fuel processing (i.e., briquetting and carbonization) could both reduce the carbonaceous fractions in $PM_{2.5}$ emitted from combustion.

K^+ was the most abundant soluble ion, with a mass proportion ranged from 2.03 to 6.84% (4.31 ± 1.59% on average). Cl^- is the next abundant soluble ion, ranging from 0.92 to 4.57% (3.05 ± 1.29% on average). Our results were consistent with those reported on other biomass burning experiments (Andreae and Merlet, 2001; Carvalho et al., 2002; Chen et al., 2017). However, large variations on mass fractions were shown for these two ions among the examined biomass fuels. The abundance of K^+ from the burning of branch-group fuels (i.e. WB, WBB and WBC) (4.78 ± 1.49%) were lower than those from herbaceous fuels (i.e. MS, MSB, MSC, WS, WSB and WSC) (3.28 ± 1.52%) ($p > 0.05$). The same results have been reported in literature, ascribed to the lower K^+ content in woody plants (Sillapapiromsuk et al., 2013). The abundance of K^+ from burning of charcoal (5.91 ± 0.92%) were significantly higher than those from burning of raw fuels (4.12 ± 1.17%) and briquette (2.80 ± 0.72%) ($p < 0.05$). It could be inferred that K^+ was enriched during carbonization as larger fractions of volatile matters and moisture had been removed. The proportions of other water-soluble ions were generally below 1% in a descending order of $SO_4^{2-} > Na^+ > NH_4^+ > Ca^{2+} > NO_3^- > Mg^{2+}$.

Besides K and Cl, the fractions of other quantified elements were low, with a sum of 2.82–4.13% to the $PM_{2.5}$ masses. The $PM_{2.5}$ from burning of charcoal had a relatively high element abundance since metals and mineral elements could not be removed efficiently during the carbonization processes. In addition, burning of branch-group fuels (3.64 ± 0.88%) had higher element abundance than herbaceous fuels burning (2.10 ± 1.17%) ($p > 0.05$). The levels of toxic heavy metals such as Cr and Ni were below detection limit, potentially attributed to all biomass fuel samples collected from human grain in origin, where the heavy metal contents were generally low in the soils (Nzihou and

Table 1
Chemical mass fraction (%) to $PM_{2.5}$ from biomass fuel burning.

Chemical	MS	MSB	MSC	WS	WSB	WSC	WB	WBB	WBC
	n = 3	n = 3	n = 3	n = 3	n = 3	n = 3	n = 3	n = 3	n = 3
OC	37.2 ± 11.3	35.3 ± 11.2	17.7 ± 0.15	39.5 ± 8.00	31.4 ± 4.9	22.2 ± 0.68	40.2 ± 3.83	30.2 ± 0.28	18.8 ± 3.09
EC	9.57 ± 0.91	9.42 ± 3.57	7.88 ± 0.53	8.82 ± 2.73	2.42 ± 0.45	1.47 ± 0.18	18.4 ± 9.27	16.2 ± 5.60	7.38 ± 4.56
Na^+	0.23 ± 0.06	0.54 ± 0.18	0.85 ± 0.24	0.53 ± 0.12	0.26 ± 0.04	0.35 ± 0.17	0.76 ± 0.21	0.70 ± 0.26	0.65 ± 0.00
NH_4^+	0.25 ± 0.02	0.16 ± 0.06	0.19 ± 0.22	0.61 ± 0.12	0.48 ± 0.02	0.12 ± 0.02	0.13 ± 0.05	1.60 ± 0.21	0.09 ± 0.04
K^+	4.23 ± 0.07	3.11 ± 2.30	6.84 ± 1.01	5.15 ± 0.77	3.37 ± 2.10	5.94 ± 0.19	2.87 ± 0.89	2.03 ± 0.17	5.01 ± 1.41
Mg^{2+}	0.02 ± 0.00	0.04 ± 0.01	0.05 ± 0.01	0.01 ± 0.00	0.02 ± 0.00	0.02 ± 0.00	0.05 ± 0.02	0.04 ± 0.02	0.04 ± 0.00
Ca^{2+}	0.22 ± 0.06	0.38 ± 0.09	0.57 ± 0.25	0.20 ± 0.08	0.24 ± 0.06	0.15 ± 0.04	0.79 ± 0.26	0.56 ± 0.17	0.31 ± 0.11
Cl-	2.80 ± 0.17	2.21 ± 1.41	4.40 ± 0.08	4.57 ± 0.19	2.78 ± 1.04	3.62 ± 0.29	1.56 ± 0.02	4.20 ± 0.96	0.92 ± 0.42
NO_3^-	0.02 ± 0.01	0.03 ± 0.01	0.13 ± 0.05	0.18 ± 0.03	0.09 ± 0.07	0.04 ± 0.01	0.09 ± 0.04	0.57 ± 0.67	0.47 ± 0.65
SO_4^{2-}	0.57 ± 0.13	0.45 ± 0.14	0.65 ± 0.04	0.72 ± 0.12	0.41 ± 0.11	0.67 ± 0.01	0.90 ± 0.19	0.77 ± 0.20	2.39 ± 0.81
Na	0.18 ± 0.02	0.89 ± 0.35	1.38 ± 0.37	0.77 ± 0.05	0.32 ± 0.22	0.26 ± 0.12	0.62 ± 0.22	0.48 ± 0.30	1.12 ± 0.11
Mg	< DL	0.04 ± 0.05	0.16 ± 0.01	0.03 ± 0.05	< DL	< DL	0.11 ± 0.16	0.04 ± 0.05	0.03 ± 0.05
Al	0.26 ± 0.13	0.32 ± 0.16	0.76 ± 0.10	0.26 ± 0.04	0.23 ± 0.08	0.12 ± 0.17	0.11 ± 0.15	0.16 ± 0.12	0.24 ± 0.04
Si	0.07 ± 0.03	0.41 ± 0.37	0.39 ± 0.30	0.09 ± 0.03	0.07 ± 0.01	0.06 ± 0.03	0.26 ± 0.05	0.20 ± 0.03	0.12 ± 0.07
S	0.71 ± 0.17	0.26 ± 0.09	0.17 ± 0.15	0.46 ± 0.11	0.33 ± 0.13	0.43 ± 0.32	0.94 ± 0.28	0.14 ± 0.13	4.43 ± 2.31
Cl	13.2 ± 4.26	17.6 ± 10.4	15.6 ± 7.03	16.4 ± 2.66	10.5 ± 5.41	6.8 ± 6.92	9.38 ± 8.99	7.18 ± 7.99	5.21 ± 0.60
K	12.8 ± 4.38	17.5 ± 11.3	14.5 ± 7.62	11.6 ± 3.55	7.82 ± 4.52	6.82 ± 6.18	11.0 ± 7.09	2.39 ± 2.01	22.2 ± 10.1
Ca	0.04 ± 0.03	0.09 ± 0.07	0.09 ± 0.06	0.01 ± 0.01	0.06 ± 0.07	0.02 ± 0.00	0.10 ± 0.03	0.02 ± 0.01	0.08 ± 0.02
Ti	< DL	< DL	0.01 ± 0	< DL	< DL	< DL	< DL	< DL	< DL
V	< DL	< DL	< DL	< DL	< DL	< DL	< DL	< DL	< DL
Cr	< DL	0.01 ± 0	0.01 ± 0	< DL	< DL	< DL	0.01 ± 0.00	0.01 ± 0.00	0.01 ± 0.00
Mn	0.01 ± 0.01	0.02 ± 0.01	0.03 ± 0.01	0.01 ± 0.00	0.01 ± 0.00	< DL	0.02 ± 0.00	0.02 ± 0.01	0.02 ± 0.01
Fe	0.03 ± 0.01	0.05 ± 0.01	0.06 ± 0.02	0.02 ± 0.01	0.03 ± 0.01	0.02 ± 0.00	0.08 ± 0.03	0.06 ± 0.01	0.04 ± 0.01
Co	< DL	< DL	< DL	< DL	< DL	< DL	< DL	< DL	< DL
Ni	< DL	< DL	< DL	< DL	< DL	< DL	< DL	< DL	< DL
Cu	0.01 ± 0.00	0.02 ± 0.01	0.03 ± 0.01	0.02 ± 0.00	0.01 ± 0.00	0.02 ± 0.01	0.03 ± 0.00	0.02 ± 0.00	0.02 ± 0.00
Zn	0.06 ± 0.03	0.49 ± 0.26	0.64 ± 0.25	0.04 ± 0.02	0.04 ± 0.03	0.07 ± 0.00	0.20 ± 0.14	0.07 ± 0.03	0.14 ± 0.01
Rb	0.01 ± 0.01	0.04 ± 0.02	0.07 ± 0.02	0.02 ± 0.01	0.01 ± 0.02	0.03 ± 0.03	0.01 ± 0.01	< DL	0.01 ± 0.00
Sb	0.02 ± 0.00	0.03 ± 0.02	0.07 ± 0.01	0.01 ± 0.00	0.02 ± 0.01	0.02 ± 0.01	0.08 ± 0.06	0.04 ± 0.03	0.05 ± 0.01
Ba	0.06 ± 0.01	0.08 ± 0.01	0.08 ± 0.02	0.04 ± 0.01	0.04 ± 0.00	0.03 ± 0.01	0.15 ± 0.01	0.09 ± 0.03	0.12 ± 0.02
Pb	0.03 ± 0.00	0.11 ± 0.03	0.18 ± 0.04	0.03 ± 0.02	0.02 ± 0.01	0.04 ± 0.03	0.11 ± 0.04	0.24 ± 0.06	0.07 ± 0.03

< DL denotes lower than detect limit.
Up to 3 significant digits were kept.

Stanmore, 2013). Unlike carbon fractions, the fuel processing could not significantly alter the ionic and elemental fractions in $PM_{2.5}$ emitted from the relevant fuels, indicating that the high abundance of K^+ (K) and Cl^- (Cl) have referential meaning for source identification.

3.2. Organic species profile

Organic species profiles on the quantified PAHs and saccharides in $PM_{2.5}$ were listed in Table 2. Their majorities of mass fractions were in 10^{-4} level, much lower than the ionic and elements. The abundance of total quantified PAHs ranged from $1.1 \pm 0.2 \times 10^{-4}$ for MS to $18.8 \pm 5.2 \times 10^{-4}$ for WS, with a descending order of raw fuels > briquette > charcoal. The $PM_{2.5}$ from charcoal burning often has a low abundance of particulate bounded-PAHs than the burnings of woody fuels or briquette ($p < 0.05$). This can be explained by more complete combustion of charcoal than raw fuels and briquettes (Oanh et al., 1999), and more important is that most of the volatile matters (> 80%) were volatilized and/or pyrolyzed during the production of charcoal. Besides, lower water content in charcoal could suppress the formation of aromatic compounds (Shen et al., 2011a,b). For individual species, the abundance of naphthalane (NAP) was all below detection limit because of its high vapor pressure (Shen et al., 2011a,b; Kong et al., 2015). Fluoranthene (FLA) and pyrene (PYR) were the two most abundant PAHs. In term of number of aromatic rings (Fig. 2), 4-rings PAHs were the dominated group. The PAHs with more aromatic rings are often associated with higher carcinogen potentials (Niu et al., 2017; Sun et al., 2018a; Xu et al., 2018). Comparably, charcoal burning showed not only lower abundance of ΣPAHs but also lower 5- and 6-ring PAHs fractions in comparison with other biomass fuels (Oanh et al., 1999), potentially suggesting less hazard to human health.

As shown in Table 2, the mass fractions of eight saccharides (at 10^{-3} level) were 1–2 orders of magnitude higher than the PAHs. Anhydrosugars (i.e. levoglucosan, mannosan and galactosan) were the top three abundant saccharides as they are products from hemicelluloses pyrolysis (Urban et al., 2014; Wang et al., 2018). Levoglucosan had the highest fraction (0.02–1.23%) to the $PM_{2.5}$ mass. The abundances of saccharides in the $PM_{2.5}$ from the biomass burning had the same descending order of raw fuels > briquette > charcoal. Most hemicelluloses pyrolysis reactions were completed during the carbonization process and therefore only trace hemicelluloses left in charcoal (Zeng et al., 2007). Characteristics on mass fraction ratio of levoglucosan/sum of saccharides (Σsaccharides) were seen for different biomass fuels. Meanwhile, briquettes had a lower levoglucosan/Σsaccharides than those of raw fuels, ascribed to the variations on combustion conditions led by density changes (Oanh et al., 1999; Shen et al., 2011a,b). The variations of saccharide fractions in three fuel forms reflect that levoglucosan might not be the best tracer for all kinds of biomass burning but is good indicator for raw biomass fuels and their briquettes.

3.3. Source diagnostic ratios

Diagnostic ratios of the chemical species can be used as source indications (Chow et al., 2004; Ni et al., 2017; Zhang et al., 2018). Table 3 compares the OC/EC and K^+/EC ratios obtained in this study and other researches. The OC/EC ratio is often applied to distinguish the combustion sources (Cao et al., 2012; Shen et al., 2007, 2010; 2011a,b), while the biomass burning had higher OC/EC ratios than coal combustion and vehicle exhaust (Cao et al., 2008; He et al., 2008; Shen et al., 2015). The OC/EC ratios in this study ranged from 1.86 ± 0.02 (for WBB) to 4.53 ± 0.70 (for WSB). The ratios for our herbaceous fuels (i.e., MS, MSB, MSC, WS, WSB and WSC) were comparable to the same types of fuels reported in Turn et al. (1997), while the values for the branch-group fuels (i.e., WB, WBB and WBC) were slightly lower than their woody fuels. Furthermore, our OC/EC ratios were much lower than those of maize straw burnt in traditional stove (22.91 ± 3.04), but were in line with the range of maize straw pellet burnt in clean stove (4.61 ± 3.42) (Sun et al., 2017). Such differences were obvious when our values were compared with those of open straw burning and residential coal/wood burning (Li et al., 2007b; Zhang et al., 2012).

Table 2
Organic profiles in $PM_{2.5}$ from biomass fuel burning ($\times 10^{-4}$ for PAHs and $\times 10^{-3}$ for Saccharide).

Organic species	MS	MSB	MSC	WS	WSB	WSC	WB	WBB	WBC
	n = 3	n = 3	n = 3	n = 3	n = 3	n = 3	n = 3	n = 3	n = 3
NAP	< DL	< DL	< DL	< DL	< DL	< DL	< DL	< DL	< DL
ACY	< DL	< DL	< DL	< DL.1	< DL	< DL	< DL	< DL	< DL
ACE	< DL	< DL	< DL	3.7 ± 1.8	< DL	< DL	< DL	0.5 ± 0.1	0.4 ± 0.2
PHE	< DL	< DL	< DL	< DL	< DL	< DL	0.6 ± 0.4	0.1 ± 0.0	< DL
ANT	< DL	< DL	< DL	< DL	< DL	< DL	0.1 ± 0.1	0.1 ± 0.0	< DL
FLA	1.0 ± 0.7	0.2 ± 0.1	0.2 ± 0.1	1.1 ± 0.1	0.6 ± 0.5	0.2 ± 0.0	1.3 ± 0.4	1.0 ± 0.2	< DL
PYR	1.5 ± 1.0	0.8 ± 0.1	0.9 ± 0.5	3.8 ± 1.7	0.9 ± 0.5	0.5 ± 0.1	2.2 ± 0.4	1.3 ± 0.1	0.8 ± 0.4
BaA	0.7 ± 0.6	< DL	< DL	1.2 ± 0.3	0.3 ± 0.3	0.1 ± 0.0	0.7 ± 0.0	0.2 ± 0.1	0.1 ± 0.0
CHR	0.9 ± 0.8	< DL	< DL	1.5 ± 0.3	0.4 ± 0.4	0.2 ± 0.0	1.0 ± 0.2	0.3 ± 0.1	0.1 ± 0.1
BbF	0.7 ± 0.5	< DL	< DL	1.4 ± 0.2	0.2 ± 0.1	0.1 ± 0.0	0.6 ± 0.0	0.2 ± 0.1	0.7 ± 0.2
BkF	0.7 ± 0.7	< DL	< DL	1.8 ± 0.3	0.2 ± 0.2	0.1 ± 0.0	0.5 ± 0.1	0.3 ± 0.1	0.1 ± 0.2
BeP	0.6 ± 0.4	< DL	< DL	1.0 ± 0.1	0.2 ± 0.1	0.1 ± 0.0	0.4 ± 0.0	0.2 ± 0.1	0.2 ± 0.1
BaP	0.6 ± 0.6	< DL	< DL	1.2 ± 0.2	0.2 ± 0.1	0.1 ± 0.0	0.5 ± 0.0	0.3 ± 0.0	0.2 ± 0.1
IcdP	0.4 ± 0.4	< DL	< DL	1.0 ± 0.1	0.1 ± 0.1	< DL	0.3 ± 0.0	0.2 ± 0.1	0.1 ± 0.1
DahA	< DL	< DL	< DL	< DL	< DL	< DL	0.4 ± 0.0	< DL	< DL
BghiP	0.5 ± 0.4	< DL	< DL	1.0 ± 0.1	0.1 ± 0.1	0.1 ± 0.0	0.1 ± 0.1	0.1 ± 0.1	0.1 ± 0.0
ΣPAHs	7.7 ± 6.0	1.1 ± 0.2	1.1 ± 0.6	18.8 ± 5.2	3.0 ± 2.4	1.6 ± 0.3	8.7 ± 1.7	4.9 ± 1.2	2.9 ± 1.3
Levoglucosan	11.7 ± 1.95	0.28 ± 0.07	0.40 ± 0.05	9.71 ± 0.67	0.86 ± 0.98	0.53 ± 0.36	3.44 ± 0.36	0.50 ± 0.71	0.03 ± 0.04
Mannosan	0.22 ± 0.04	0.01 ± 0.00	0.12 ± 0.01	0.21 ± 0.01	0.04 ± 0.05	0.20 ± 0.14	0.22 ± 0.02	0.03 ± 0.04	0.01 ± 0.01
Galactosan	0.32 ± 0.05	0.01 ± 0.00	0.15 ± 0.02	0.20 ± 0.01	0.06 ± 0.06	0.12 ± 0.08	0.18 ± 0.02	0.02 ± 0.03	0.01 ± 0.01
arabitol	1.97 ± 0.44	0.02 ± 0.00	0.02 ± 0.03	0.02 ± 0.00	0.04 ± 0.05	0.02 ± 0.02	0.18 ± 0.04	0.03 ± 0.04	< DL
D-glucose	0.01 ± 0.00	< DL	< DL	0.06 ± 0.02	< DL	< DL	< DL	< DL	< DL
mannitol	0.05 ± 0.01	< DL	< DL	0.01 ± 0.00	< DL	< DL	0.22 ± 0.07	< DL	< DL
inositol	0.05 ± 0.01	0.00 ± 0.01	< DL	< DL	< DL	0.00 ± 0.01	< DL	< DL	< DL
sucrose	0.06 ± 0.02	0.07 ± 0.02	0.02 ± 0.01	< DL	0.03 ± 0.02	0.02 ± 0.01	0.08 ± 0.11	0.05 ± 0.07	< DL
ΣSaccharide	14.3 ± 2.52	0.40 ± 0.11	0.34 ± 0.11	10.2 ± 0.74	1.03 ± 1.17	0.89 ± 0.62	4.33 ± 0.62	0.64 ± 0.91	0.04 ± 0.06

< DL denotes below detection limit.
Up to 3 significant digits were kept.

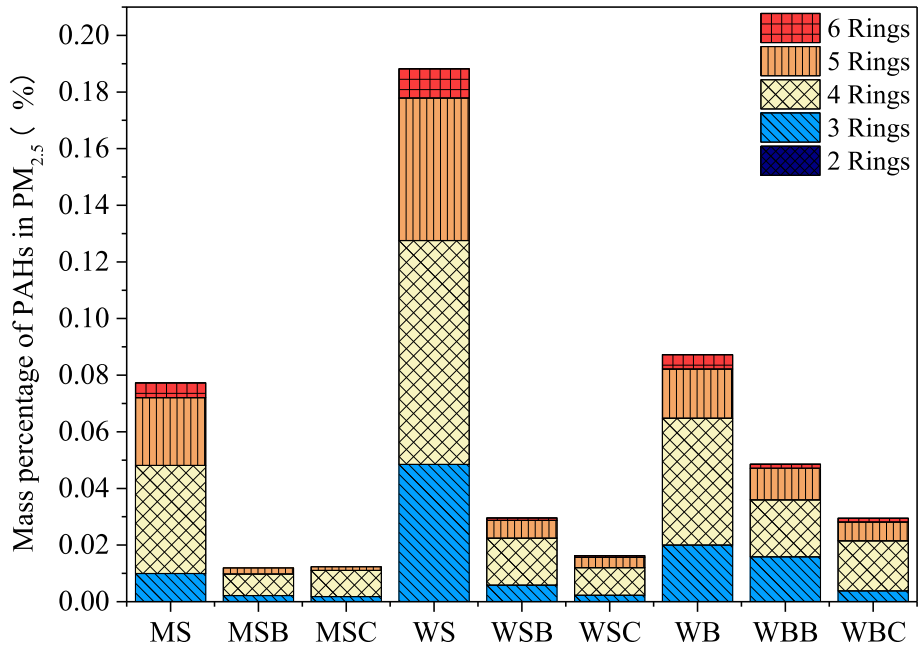

Fig. 2. Mass fractions of PAHs in term of number of aromatic rings.

Table 3
Comparison of ratios of OC/EC and K^+/EC for biomass fuel emissions.

$PM_{2.5}$ source	OC/EC	K^+/EC	Reference
MS	3.89 ± 1.18	0.44 ± 0.01	This study
MSB	3.75 ± 1.19	0.33 ± 0.24	
MSC	2.24 ± 0.02	0.87 ± 0.13	
WS	4.47 ± 0.9	0.58 ± 0.09	
WSB	4.53 ± 0.7	0.49 ± 0.03	
WSC	3.63 ± 0.11	0.97 ± 0.03	
WB	2.19 ± 0.21	0.16 ± 0.05	
WBB	1.86 ± 0.02	0.13 ± 0.01	
WBC	2.54 ± 0.42	0.68 ± 0.19	
Herbaceous fuels	3.22 ± 0.11	0.78 ± 0.12	Turn et al. (1997)
Woody fuels	3.86 ± 0.21	0.19 ± 0.01	
Maize straw open burning	5.51 ± 2.01	2.29 ± 1.32	Li et al. (2007)
Wheat straw open burning	11.14 ± 4.85	0.94 ± 0.41	
Maize straw in traditional stove	22.91 ± 3.04	1.16 ± 0.34	Sun et al. (2017)
Maize straw in clean stove	13.05 ± 1.22	1.38 ± 0.54	
Maize straw pellet in clean stove	4.61 ± 3.42	–	

The ratio of K^+/EC has been adopted to assess biomass burning contributions (Shen et al., 2009). In this study, the herbaceous fuels showed comparable K^+/EC ratios with those reported in Turn et al. (1997) but were lower than those in open straw burning (Li et al., 2007b; Ni et al., 2017). The K^+/EC ratios for WB and WBB were also consistent with those of woody fuels shown in Turn et al. (1997) but was ~4 times the values for charcoals (i.e., WBC) found in this study. It should be noted that the K^+/EC ratios from charcoal were 2–5 times higher than those of briquette. This might act as a good indicator for distinguishing the $PM_{2.5}$ emitted from burning of charcoal and briquette fuels.

The diagnostic ratios of saccharides can also act as indicators to discriminate the combustion sources (Schmidl et al., 2008) (Table 4). The ratios of Σsaccharides to $PM_{2.5}$ varied dramatically from 0.0041% to 1.4%, representing a four order of magnitude differences between WBC to MS. The ratios of Σsaccharides/$PM_{2.5}$ for raw fuels were much higher than those for briquette and charcoal. However, the low Σsaccharides/$PM_{2.5}$ for briquette and charcoal were close to the values of other pollution sources, such as agricultural soil dust (0.004 ± 0.007), road dust (0.012 ± 0.020) and ambient aerosol (0.20 ± 0.25). Hence, it could not be properly applied in source identification (Jia and Fraser, 2011). The carbon ratio of Σsaccharides to OC were consistent with the mass ratio of Σsaccharides/$PM_{2.5}$, only 10–20% higher in values, suggesting that the average molecular weight of OM were lower than those of saccharides in $PM_{2.5}$.

The ratios of levoglucosan to mannosan for MS and WS were 52 and 46, respectively, close to the range of 33–97 reported in literature (Sheesley et al., 2003). The fuel samples of MSB, WSB, WB and WBB had close levoglucosan/mannosan ratios (in a range of 15–19), also

Table 4
Diagnostic ratios of saccharides.

	Σsaccharide/$PM_{2.5}$ (x10^{-2})	Carbon in Σsaccharide/OC (x10^{-2})	Levoglucosan/Σsaccharide	Levoglucosan/mannosan	Levoglucosan/galatcosan
MS	1.4	1.7	0.81	52	37
MSB	0.040	0.052	0.69	19	20
MSC	0.037	0.083	0.53	3.3	2.6
WS	1.0	1.2	0.95	46	49
WSB	0.10	0.15	0.83	19	15
WSC	0.091	0.18	0.60	2.7	4.5
WB	0.43	0.47	0.79	15	19
WBB	0.064	0.094	0.78	17	21.
WBC	0.0041	0.0097	0.65	4.2	3.4

*Two significant figures are given.

Table 5
A summary on distribution of chemical composition to $PM_{2.5}$ mass (wt % of $PM_{2.5}$ mass).

Biomass fuels	> 10%	1–10%	0.1–1%	0.01–0.1%	< 0.01%
MS	OC	EC, K^+, Cl^-, K, Cl, Levoglucosan	Na^+, NH_4^+, Ca^{2+}, SO_4^{2-}, Na, Al, S, arbaitol	Mg^{2+}, NO_3^-, Si, Ca, Fe, Zn, Rb, Sb, Ba, Pb, Mannosan, Galatcosan, FLA	Ti, V, Cr, Mn, Co, Ni, Cu, D-glucose, mannitol, inositol, sucrose, NAP, ACY, ACE, FLO, PHE, ANT, PYR, BaA, CHR, BbF, BkF, BaP, IcdP, DahA, BghiP
MSB	OC	EC, K^+, Cl^-, K, Cl	Na^+,NH_4^+, Ca^{2+}, SO_4^{2-}, Na, Al, Si, S, Zn, Pb	Mg^{2+}, NO_3^-, Mg, Ca, Cr, Mn, Fe, Cu, Rb, Sb, Ba, Levoglucosan	Ti, V, Cr, Co, Ni, Mannosan, D-glucose, mannitol, inositol, sucrose, arbaitol, Galatcosan, NAP, ACY, ACE, FLO, PHE, ANT, FLA, PYR, BaA, CHR, BbF, BkF, BaP, IcdP, DahA, BghiP
MSC	OC	EC, K^+, Cl^-, K, Cl, Na,	Na^+, NH_4^+, Ca^{2+}, NO_3^-, SO_4^{2-}, Mg, Al, Si, S, Zn, Pb, Levoglucosan	Mg^{2+}, Ca, Cr, Mn, Fe, Cu, Rb, Sb, Ba	Ti, V, Co, Ni, Mannosan, D-glucose, mannitol, inositol, sucrose, arbaitol, Galatcosan, NAP, ACY, ACE, FLO, PHE, ANT, FLA, PYR, BaA, CHR, BbF, BkF, BaP, IcdP, DahA, BghiP
WS	OC	EC, K^+, Cl^-, K, Cl	Na^+,NH_4^+, Ca^{2+}, NO_3^-, SO_4^{2-}, Na, Al, S	Mg^{2+}, Mg, Si, Ca, Fe, Cu, Zn, Rb, Sb, Ba, Pb, Levoglucosan, Mannosan, Galatcosan, ACE, ANT, FLA, PYR, BaA, CHR, BbF, BkF, BaP, IcdP, BghiP	Ti, V, Cr, Mn, Co, Ni, D-glucose, mannitol, inositol, sucrose, arbaitol, NAP, ACY, FLO, PHE, DahA
WSB	OC	EC, K^+, Cl^-, K, Cl	Na^+, NH_4^+, Ca^{2+}, SO_4^{2-}, Na, Al, S	Mg^{2+}, NO_3^-, Si, Ca, Fe, Cu, Zn, Rb, Sb, Ba, Pb, Levoglucosan	Ti, V, Cr, Mn, Co, Ni, Mannosan, D-glucose, mannitol, inositol, sucrose, arbaitol, Galatcosan, NAP, BaA, CHR, BbF, BkF, BaP, IcdP, DahA, BghiP ACY, ACE, FLO, PHE, ANT, FLA, PYR, BaA, CHR, BbF, BkF, BaP, IcdP, DahA, BghiP
WSC	OC	EC, K^+, Cl^-, K, Cl	Na^+, NH_4^+, Ca^{2+}, SO_4^{2-}, Na, Al, S	Mg^{2+}, NO_3^-, Si, Ca, Fe, Cu, Zn, Rb, Sb, Ba, Pb, Galatcosan	Ti, V, Cr, Mn, Co, Ni, Mannosan, D-glucose, mannitol, inositol, sucrose, arbaitol, NAP, ACY, ACE, FLO, PHE, ANT, FLA, PYR, BaA, CHR, BbF, BkF, BaP, IcdP, DahA, BghiP
WB	OC, EC	K^+, Cl^-, K, Cl	Na^+, NH_4^+, Ca^{2+}, SO_4^{2-}, Na, Mg, Al, Si, S, Ca, Zn, Ba, Pb, Levoglucosan	Mg^{2+}, NO_3^-, Cr, Mn, Fe, Cu, Sb, Mannosan, mannitol, arbaitol, Galatcosan, ANT, FLA	Ti, V, Co, Ni, Rb, D-glucose, inositol, sucrose, NAP, ACY, ACE, FLO, PHE, PYR, BaA, CHR, BbF, BkF, BaP, IcdP, DahA, BghiP
WBB	OC, EC	NH_4^+, K^+, Cl^-, K, Cl	Na^+, Ca^{2+}, NO_3^-, SO_4^{2-}, Na, Al, Si, S, Pb	Mg^{2+}, Mg, Ca, Mn, Fe, Cu, Zn, Sb, Ba, Levoglucosan, FLA	Ti, V, Cr, Co, Ni, Rb, Mannosan, D-glucose, mannitol, inositol, sucrose, arbaitol, Galatcosan, NAP, ACY, ACE, FLO, PHE, ANT, PYR, BaA, CHR, BbF, BkF, BaP, IcdP, DahA, BghiP
WBC	OC	EC, K^+, SO_4^{2-}, Na, S, K, Cl	Na^+, Cl^-, NH_4^+, Ca^{2+}, NO_3^-, SO_4^{2-}, Al, Si, Zn, Ba	Mg^{2+}, Mg, Ca, Mn, Fe, Cu, Sb, Pb	Ti, Cr, Co, Ni, Rb, Levoglucosan, Mannosan, D-glucose, mannitol, inositol, sucrose, arbaitol, Galatcosan, NAP, ACY, ACE, FLO, PHE, ANT, FLA, PYR, BaA, CHR, BbF, BkF, BaP, IcdP, DahA, BghiP

Table 6
Coefficient of divergence on the chemical profiles in this study[a].

	MS	MSB	MSC	WS	WSB	WSC	WB	WBB	WBC
MS	0								
MSB	0.36	0							
MSC	0.47	0.26	0						
WS	0.29	0.42	0.47	0					
WSB	0.21	0.37	0.46	0.22	0				
WSC	0.25	0.41	0.49	0.26	0.26	0			
WB	0.40	0.28	0.33	0.45	0.47	0.45	0		
WBB	0.45	0.42	0.43	0.43	0.42	0.47	0.40	0	
WBC	0.41	0.37	0.40	0.45	0.43	0.47	0.44	0.30	0

[a] The chemical profiles combines regular and organic profiles.

consistent with an average of 15 reported in Schmidl et al. (2008). Furthermore, charcoal had much lower ratios of levoglucosan/mannosan (2.7–4.2), also comparable with the results from softwood burning (Schmidl et al., 2008). Conclusively, the ratios of levoglucosan/galactosan and levoglucosan/Σsaccharide can resemble the same features as ratio of levoglucosan/mannosan in identification of biomass burning. Based on the ranges of ratios, three characteristic groups can be clearly divided, namely straws (i.e., MS and WS), woods (i.e., MSB, WSB, WB and WBB) and charcoal (i.e., MSC, WSC and WBC). It should be also noted that straw briquettes had very close properties as the wood branches due to the content of volatile matter and density (Zeng et al., 2007).

3.4. Similarity analysis

A summary on the distributions of chemical species was shown in Table 5. OC is the most abundant component, with a range of mass fractions in $PM_{2.5}$ of 17.65 ± 0.15% for MSC and 40.17 ± 3.83% for WB (Ni et al., 2017; Turn et al., 1997; Watson et al., 2001). The ions of K^+ (Cl^-) and elemental of K (Cl) contributed 1–10% of $PM_{2.5}$ masses (Ni et al., 2017; Sillapapiromsuk et al., 2013; Zhang et al., 2018). Previous studies commonly reported high emissions of K^+ and Cl^- from biomass fuel burning, while the variations on their abundances could be subjected to fuel composition and combustion temperatures (Hays et al., 2005; McMeeking et al., 2009; Oanh et al., 2011; Sun et al., 2017). The results of this study further prove that the form of biomass fuels is a crucial factor for the emission of either K^+ (Cl^-) or K (Cl). Other soluble ions had mass fractions ranged from 0.1 to 1%, but at least one magnitude lower in mass fractions (0.01–0.1%) were seen for the trace elements (i.e., heavy metals). For the organic species, the mass fractions of anhydrosugars ranged from 0.01 to 0.1%. Other individual saccharides and priority PAHs were < 0.01% or even below the detection limit. Dissimilar with the homogeneous features, obvious variations on EC were found, with the highest and lowest mass fractions for WB (18.35 ± 9.27%) and WSC (1.47 ± 0.18%), respectively. The largest variation on mass fraction was found for levoglucosan, a maximum factor of ~400 between WBC (0.03 ± 0.04%) and MS (11.65 ± 1.95%).

The similarity of chemical profiles for the different bio-fuels burning were accessed by calculating the coefficient of divergence (CD) and their correlations (Table 6 and S4). Generally, the fuels of MS, MSB, WS and WSB had similar profiles with CDs ranged from 0.21 to 0.36 (R > 0.97). Ni et al. (2017) found that agricultural straws burning could be classified into the same category in source apportionment as the low CDs and high correlation. This conclusion could be also applicable for maize and wheat straws and their briquettes. The CD values between charcoal and their raw fuels were generally greater than those between briquettes and corresponding raw fuels, particularly for maize straw and branch-groups. In addition, both CDs between MS and MSC (0.47, R = 0.79) and between WB and WBC (0.44, R = 0.69) indicate significant differences in the profiles of charcoal and its raw fuels. At the same time, different types of charcoal could not be simply deemed as the same source because of their relatively high CD (0.40–0.49) and high R (0.83–0.90). In summary, woody and herbaceous fuels should be considered separately, whereas charcoal produced from different raw fuels must be also classified as individual sub-categories due to the high CD values among their chemical profiles.

4. Conclusion

Chemical source profiles for different biomass burning were investigated in this study. The results were consistent with those reported in the literature. The organic profiles and their diagnosis ratios provide more informative features to distinguish the combustion sources. Demonstrated by the unique mass fractions of chemicals for charcoal, the processing such as carbonization on raw biomass materials could impact the natures of fuels and emission of $PM_{2.5}$ significantly. Hence, those factors must be taken into account for building emission inventories on biomass burning and conducting source apportionment.

Acknowledgement

This research was supported by the National Key R&D Program of China (2017YFC0212205), the Natural Science Foundation of Shaanxi Province, China (2016ZDJC-22), and two grants from SKLLQG, Chinese Academy of Sciences (SKLLQG1616 and SKLLQG1826).

Appendix A. Supplementary data

Supplementary data to this article can be found online at https://doi.org/10.1016/j.atmosenv.2019.02.038.

References

Andreae, M.O., Merlet, P., 2001. Emission of trace gases and aerosols from biomass burning. Glob. Biogeochem. Cycles 15, 955–966.
Bi, X., Simoneit, B.R.T., Sheng, G., Ma, S., Fu, J., 2008. Composition and major sources of organic compounds in urban aerosols. Atmos. Res. 88, 256–265.
Cao, J.J., Lee, S.C., Chow, J.C., Watson, J.G., Ho, K.F., Zhang, R.J., Jin, Z.D., Shen, Z.X., Chen, G.C., Kang, Y.M., Zou, S.C., Zhang, L.Z., Qi, S.H., Dai, M.H., Cheng, Y., Hu, K., 2007. Spatial and seasonal distributions of carbonaceous aerosols over China. J. Geophys. Res.: Atmosphere 112.
Cao, G., Zhang, X., Gong, S., Zheng, F., 2008. Investigation on emission factors of particulate matter and gaseous pollutants from crop residue burning. J. Environ. Sci. 20, 50–55.
Cao, J.J., Shen, Z.X., Chow, J.C., Watson, J.G., Lee, S.C., Tie, X.X., Ho, K.F., Wang, G.H., Han, Y.M., 2012. Winter and summer PM2.5 chemical compositions in fourteen Chinese cities. J. Air Waste Manag. Assoc. 62, 1214–1226.
Carvalho, E.R., Gurgel Veras, C.A., CarvalhoJr, J.A., 2002. Experimental investigation of smouldering in biomass. Biomass Bioenergy 22, 283–294.
Chen, J., Li, C., Ristovski, Z., Milic, A., Gu, Y., Islam, M.S., Wang, S., Hao, J., Zhang, H., He, C., Guo, H., Fu, H., Miljevic, B., Morawska, L., Thai, P., Lam, Y.F., Pereira, G., Ding, A., Huang, X., Dumka, U.C., 2017. A review of biomass burning: emissions and impacts on air quality, health and climate in China. Sci. Total Environ. 579, 1000–1034.
Chow, J.C., Watson, J.G., Kuhns, H., Etyemezian, V., Lowenthal, D.H., Crow, D., Kohl, S.D., Engelbrecht, J.P., Green, M.C., 2004. Source profiles for industrial, mobile, and area sources in the big bend regional aerosol visibility and observational study. Chemosphere 54, 185–208.
Chow, J.C., Watson, J.G., Chen, L.-W.A., Chang, M.O., Robinson, N.F., Trimble, D., Kohl, S., 2007. The IMPROVE_A temperature protocol for thermal/optical carbon analysis: maintaining consistency with a long-term database. J. Air Waste Manag. Assoc. 57, 1014–1023.
Chow, J.C., Lowenthal, D.H., Chen, L.W.A., Wang, X., Watson, J.G., 2015. Mass reconstruction methods for PM2.5: a review. Air Quality, Atmosphere & Health 8, 243–263.
Han, Y.M., Cao, J.J., Lee, S.C., Ho, K.F., An, Z.S., 2010. Different characteristics of char and soot in the atmosphere and their ratio as an indicator for source identification in Xi'an, China. Atmos. Chem. Phys. 10, 595–607.
Hays, M.D., Fine, P.M., Geron, C.D., Kleeman, M.J., Gullett, B.K., 2005. Open burning of agricultural biomass: physical and chemical properties of particle-phase emissions. Atmos. Environ. 39, 6747–6764.
He, L.Y., Hu, M., Zhang, Y.H., Huang, X.F., Yao, T.T., 2008. Fine particle emissions from on-road vehicles in the Zhujiang Tunnel, China. Environ. Sci. Technol. 42, 4461–4466.
Jia, Y., Fraser, M., 2011. Characterization of saccharides in size-fractionated ambient

particulate matter and aerosol sources: the contribution of primary biological aerosol particles (PBAPs) and soil to ambient particulate matter. Environ. Sci. Technol. 45, 930–936.
Kong, S.F., Ding, X., Bai, Z.P., Han, B., Chen, L., Shi, J.W., Li, Z.Y., 2010. A seasonal study of polycyclic aromatic hydrocarbons in PM2.5 and PM2.5–10 in five typical cities of Liaoning Province, China. J. Hazard Mater. 183, 70–80.
Kong, S.F., Ji, Y.Q., Li, Z.Y., Lu, B., Bai, Z.P., 2013. Emission and profile characteristic of polycyclic aromatic hydrocarbons in PM2.5 and PM10 from stationary sources based on dilution sampling. Atmos. Environ. 77, 155–165.
Kong, S.F., Li, X.X., Li, L., Yin, Y., Chen, K., Yuan, L., Zhang, Y.J., Shan, Y.P., Ji, Y.Q., 2015. Variation of polycyclic aromatic hydrocarbons in atmospheric PM2.5 during winter haze period around 2014 Chinese Spring Festival at Nanjing: insights of source changes, air mass direction and firework particle injection. Sci. Total Environ. 520, 59–72.
Li, X., Wang, S., Duan, L., Hao, J., Li, C., Chen, Y., Yang, L., 2007. Particulate and trace gas emissions from open burning of wheat straw and corn stover in China. Environ. Sci. Technol. 41, 6052–6058.
Li, X.H., Duan, L., Wang, S.X., Duan, J., Guo, X., Yi, H., Hu, J., Li, C., Hao, J.M., 2007a. Emission characteristics of particulate matter from rural household biofuel combustion in China. Energy Fuels 21, 845–851.
Li, X.H., Wang, S.X., Duan, L., Hao, J.M., Li, C., Chen, Y.S., Yang, L., 2007b. Particulate and trace gas emissions from open burning of wheat straw and corn stover in China. Environ. Sci. Technol. 41, 6052–6058.
Li, X., Chen, M., Le, H.P., Wang, F., Guo, Z., Iinuma, Y., Chen, J., Herrmann, H., 2016. Atmospheric outflow of PM2.5 saccharides from megacity Shanghai to East China Sea: impact of biological and biomass burning sources. Atmos. Environ. 143, 1–14.
Liu, J.Y., Zhai, G.X., Chen, R.Y., 2001. Analysis on the characteristics of biomass fuel direct combustion process. J. Northeast Agric. Univ. 03.
McMeeking, G.R., Kreidenweis, S.M., Baker, S., Carrico, C.M., Chow, J.C., Collett, J.L., Hao, W.M., Holden, A.S., Kirchstetter, T.W., Malm, W.C., 2009. Emissions of trace gases and aerosols during the open combustion of biomass in the laboratory. J. Geophys. Res.: Atmosphere 114 1984–2012.
Medeiros, P.M., Conte, M.H., Weber, J.C., Simoneit, B.R.T., 2006. Sugars as source indicators of biogenic organic carbon in aerosols collected above the Howland Experimental Forest, Maine. Atmos. Environ. 40, 1694–1705.
Mo, Z., Shao, M., Lu, S., 2016. Compilation of a source profile database for hydrocarbon and OVOC emissions in China. Atmos. Environ. 143, 209–217.
Ni, H.Y., Han, Y.M., Cao, J.J., Chen, L.-W.A., Tian, J., Wang, X.L., Chow, J.C., Watson, J.G., Wang, Q.Y., Wang, P., 2015. Emission characteristics of carbonaceous particles and trace gases from open burning of crop residues in China. Atmos. Environ. 123, 399–406.
Ni, H.Y., Tian, J., Wang, X.L., Wang, Q.Y., Han, Y.M., Cao, J.J., Long, X., Chen, L.W.A., Chow, J.C., Watson, J.G., Huang, R.J., Dusek, U., 2017. $PM_{2.5}$ emissions and source profiles from open burning of crop residues. Atmos. Environ. 169, 229–237.
Niu, X.Y., Ho, S.S.H., Ho, K.F., Huang, Y., Sun, J., Wang, Q.Y., Zhou, Y.Q., Zhao, Z.Z., Cao, J.J., 2017. Atmospheric levels and cytotoxicity of polycyclic aromatic hydrocarbons and oxygenated-PAHs in PM2.5 in the Beijing-Tianjin-Hebei region. Environ. Pollut. 231, 1075–1084.
Nzihou, A., Stanmore, B., 2013. The fate of heavy metals during combustion and gasification of contaminated biomass—a brief review. J. Hazard Mater. 256–257, 56–66.
Oanh, N.T.K., Reutergardh, L.B., Dung, N.T., 1999. Emission of polycyclic aromatic hydrocarbons and particulate matter from domestic combustion of selected fuels. Environ. Sci. Technol. 33, 2703–2709.
Oanh, N.T.K., Ly, B.T., Tipayarom, D., Manandhar, B.R., Prapat, P., Simpson, C.D., Liu, L.-J.S., 2011. Characterization of particulate matter emission from open burning of rice straw. Atmos. Environ. 45, 493–502.
Ravichandran, P., Corscadden, K., 2014. Comparison of gaseous and particle emissions produced from leached and un-leached agricultural biomass briquettes. Fuel Process. Technol. 128, 359–366.
Robinson, A.L., Subramanian, R., Donahue, N.M., Bernardo-Bricker, A., Rogge, W.F., 2006. Source apportionment of molecular markers and organic aerosol. 2. Biomass smoke. Environ. Sci. Technol. 40, 7811–7819.
Schmidl, C., Marr, I.L., Caseiro, A., Kotianová, P., Berner, A., Bauer, H., Kasper-Giebl, A., Puxbaum, H., 2008. Chemical characterisation of fine particle emissions from wood stove combustion of common woods growing in mid-European Alpine regions. Atmos. Environ. 42, 126–141.
Sheesley, R.J., Schauer, J.J., Chowdhury, Z., Cass, G.R., Simoneit, B.R.T., 2003. Characterization of organic aerosols emitted from the combustion of biomass indigenous to South Asia. J. Geophys. Res.: Atmosphere 108.
Sheesley, R.J., Schauer, J.J., Zheng, M., Wang, B., 2007. Sensitivity of molecular marker-based CMB models to biomass burning source profiles. Atmos. Environ. 41, 9050–9063.
Shen, Z., Cao, J., Arimoto, R., Zhang, R., Jie, D., Liu, S., Zhu, C., 2007. Chemical composition and source characterization of spring aerosol over Horqin sand land in northeastern China. J. Geophys. Res. 112, D14315.
Shen, Z.X., Cao, J.J., Arimoto, R., Han, Z., Zhang, R.J., Han, Y.M., Liu, S.X., Okuda, T., Nakao, S., Tanaka, S., 2009. Ionic composition of TSP and $PM_{2.5}$ during dust storms and air pollution episodes at Xi'an, China. Atmos. Environ. 43, 2911–2918.
Shen, Z.X., Cao, J.J., Arimoto, R., Han, Y.M., Zhu, C.S., Tian, J., Liu, S.X., 2010. Chemical characteristics of fine particles (PM_1) from xi'an, China. Aerosol Sci. Technol. 44 (6), 461–472.
Shen, G.F., Wei, W., Yang, Y.F., Ding, J.N., Xue, M., Min, Y.J., 2011a. Emissions of PAHs from indoor crop residue burning in a typical rural stove: emission factors, size distributions, and gas-particle partitioning. Environ. Sci. Technol. 45, 1206–1212.
Shen, Z., Cao, J., Liu, S., Zhu, C., Wang, X., Zhang, T., Xu, H., Hu, T., 2011b. Chemical composition of PM_{10} and $PM_{2.5}$ collected at ground level and 100 meters during a strong winter-time pollution episode in Xi'an, China. J. Air Waste Manag. Assoc. 61 (11), 1150–1159.
Shen, G.F., Wei, S.Y., Wei, W., Zhang, Y.Y., Min, Y.J., Wang, B., Wang, R., Li, W., Shen, H.Z., Huang, Y., Yang, Y., Wang, W., Wang, X., Wang, X., Tao, S., 2012. Emission factors, size distributions, and emission inventories of carbonaceous particulate matter from residential wood combustion in rural China. Environ. Sci. Technol. 46, 4207–4214.
Shen, G.F., Tao, S., Wei, S., Chen, Y.C., Zhang, Y.Y., Shen, H.Z., Huang, Y., Zhu, D., Yuan, C.Y., Wang, H.C., Wang, Y.F., Pei, L.J., Liao, Y.L., Duan, Y.H., Wang, B., Wang, R., Lv, Y., Li, W., Wang, X.L., Zheng, X.Y., 2013. Field measurement of emission factors of PM, EC, OC, parent, nitro-, and oxy- polycyclic aromatic hydrocarbons for residential briquette, coal cake, and wood in rural shanxi, China. Environ. Sci. Technol. 47, 2998–3005.
Shen, G.F., Chen, Y.C., Xue, C.Y., Lin, N., Huang, Y., Shen, H.Z., Wang, Y.L., Li, T.C., Zhang, Y.Y., Su, S., 2015. Pollutant emissions from improved coal-and wood-fuelled cookstoves in rural households. Environ. Sci. Technol. 45, 6590–6598.
Shen, Z.X., Sun, J., Cao, J.J., Zhang, L.M., Zhang, Q., Lei, Y.L., Cao, J.J., Huang, R.J., Liu, S.X., Huang, Y., Zhu, C.S., Xu, H.M., Zheng, C.L., Liu, P.P., Xue, Z.G., 2016. Chemical profiles of urban fugitive dust $PM_{2.5}$ samples in Northern Chinese cities. Sci. Total Environ. 569, 619–626.
Sillapapiromsuk, S., Chantara, S., Tengjaroenkul, U., Prasitwattanaseree, S., Prapamontol, T., 2013. Determination of PM10 and its ion composition emitted from biomass burning in the chamber for estimation of open burning emissions. Chemosphere 93, 1912–1919.
Simoneit, B.R.T., Schauer, J.J., Nolte, C.G., Oros, D.R., Elias, V.O., Fraser, M.P., Rogge, W.F., Cass, G.R., 1999. Levoglucosan, a tracer for cellulose in biomass burning and atmospheric particles. Atmos. Environ. 33, 173–182.
Sun, J., Shen, Z.X., Cao, J.J., Zhang, L.M., Wu, T.T., Zhang, Q., Yin, X.L., Lei, Y.L., Huang, Y., Huang, R.J., Liu, S.X., Han, Y.M., Xu, H.M., Zheng, C.L., Liu, P.P., 2017. Particulate matters emitted from maize straw burning for winter heating in rural areas in Guanzhong Plain, China: current emission and future reduction. Atmos. Res. 184, 66–76.
Sun, J., Shen, Z.X., Zeng, Y.L., Niu, X.Y., Wang, J., Cao, J.J., Gong, X.S., Xu, H.M., Wang, T., Liu, H.X., Yang, L., 2018a. Characterization and cytotoxicity of PAHs in PM2.5 emitted from residential solid fuel burning in the Guanzhong Plain, China. Environ. Pollut. 241, 359–368.
Sun, J., Shen, Z.X., Zhang, L.M., Zhang, Q., Lei, Y.L., Cao, J.J., Huang, Y., Liu, S., Zheng, C.L., Xu, H.M., 2018b. Impact of primary and secondary air supply intensity in stove on emissions of size-segregated particulate matter and carbonaceous aerosols from apple tree wood burning. Atmos. Res. 202, 33–39.
Sun, J., Shen, Z.X., Zhang, L.M., Lei, Y.L., Gong, X.S., Zhang, Q., Zhang, T., Xu, H.M., Cui, S., Wang, Q.Y., Cao, J.J., Tao, J., Zhang, N.N., Zhang, R., 2019. Chemical source profiles of urban fugitive dust $PM_{2.5}$ samples from 21 cities across China. Sci. Total Environ. 649, 1045–1053.
Tao, S., Li, B.G., Zhang, Y.X.X., Yuan, H.S., 2011. Emission of polycyclic aromatic hydrocarbons in China, biophysico-chemical processes of anthropogenic organic compounds. Environmental Systems. https://doi.org/10.1002/9780470944479.ch11.
Tao, J., Zhang, L., Zhang, R., Huang, R., Zhang, Z., Cao, J., Zhang, Y., 2015. Uncertainty assessment of source attribution of $PM_{2.5}$ and its water-soluble organic carbon content using different biomass burning tracers in positive matrix factorization analysis - a case study in Beijing. Sci. Total Environ. 543, 326–335.
Tian, J., Chow, J.C., Cao, J.J., Han, Y.M., Ni, H.Y., Chen, L.-W.A., Wang, X.L., Huang, R.J., Moosmüller, H., Watson, J.G., 2015. A biomass combustion chamber: design, evaluation, and a case study of wheat straw combustion emission tests. Aerosol and Air Quality Research 15, 2104–2114.
Turn, S., Jenkins, B., Chow, J., Pritchett, L., Campbell, D., Cahill, T., Whalen, S., 1997. Elemental characterization of particulate matter emitted from biomass burning: Wind tunnel derived source profiles for herbaceous and wood fuels. J. Geophys. Res.: Atmosphere 102, 3683–3699 1984–2012.
Urban, R.C., Alves, C.A., Allen, A.G., Cardoso, A.A., Queiroz, M.E.C., Campos, M.L.A.M., 2014. Sugar markers in aerosol particles from an agro-industrial region in Brazil. Atmos. Environ. 90, 106–112.
Wang, X., Chow, J.C., Kohl, S.D., Percy, K.E., Legge, A.H., Watson, J.G., 2015. Characterization of PM2.5 and PM10 fugitive dust source profiles in the athabasca oil sands region. J. Air Waste Manag. Assoc. 65, 1421–1433.
Wang, X., Shen, Z.X., Liu, F.B., Lu, D., Tao, J., Lei, Y.L., Zhang, Q., Zeng, Y.L., Xu, H.M., Wu, Y., Zhang, R., Cao, J.J., 2018. Saccharides in summer and winter PM2.5 over Xi'an, Northwestern China: sources, and yearly variations of biomass burning contribution to $PM_{2.5}$. Atmos. Res. 214, 410–417.
Watson, J.G., Chow, J.C., Houck, J.E., 2001. $PM_{2.5}$ chemical source profiles for vehicle exhaust, vegetative burning, geological material, and coal burning in Northwestern Colorado during 1995. Chemosphere 43, 1141–1151.
Xu, S., Liu, W., Tao, S., 2006. Emission of polycyclic aromatic hydrocarbons in China. Environ. Sci. Technol. 40, 702–708.
Xu, H.M., Li, Y., Guinot, B., Wang, J., He, K., Ho, K.F., Cao, J.J., Shen, Z.X., Sun, J., Lei, Y.L., Gong, X.S., Zhang, T., 2018. Personal exposure of $PM_{2.5}$ emitted from solid fuels combustion for household heating and cooking in rural Guanzhong Plain, northwestern China. Atmos. Environ. 185, 196–206.
Zeng, X.Y., Ma, Y.T., Ma, L.R., 2007. Utilization of straw in biomass energy in China. Renew. Sustain. Energy Rev. 11, 976–987.
Zhang, H., Wang, S., Hao, J., Wan, L., Jiang, J., Zhang, M., Mestl, H.E.S., Alnes, L.W.H., Aunan, K., Mellouki, A.W., 2012. Chemical and size characterization of particles emitted from the burning of coal and wood in rural households in Guizhou, China. Atmos. Environ. 51, 94–99.
Zhang, Y., Shao, M., Lin, Y., Luan, S., Mao, N., Chen, W., Wang, M., 2013. Emission inventory of carbonaceous pollutants from biomass burning in the Pearl River Delta

Region, China. Atmos. Environ. 76, 189–199.
Zhang, Q., Shen, Z.X., Cao, J.J., Ho, K.F., Zhang, R., Bie, Z.J., Chang, H., Liu, S.X., 2014a. Chemical profiles of urban fugitive dust over Xi'an in the south margin of the Loess Plateau, China. Atmospheric Pollution Research 5.
Zhang, R., Cao, J.J., Tang, Y., Arimoto, R., Shen, Z.X., Wu, F., Han, Y.M., Wang, G.H., Zhang, J., Li, G.H., 2014b. Elemental profiles and signatures of fugitive dusts from Chinese deserts. Sci. Total Environ. 472, 1121–1129.
Zhang, Y., Tian, J., Shen, Z.X., Wang, W.J., Ni, H.Y., Liu, S.X., Cao, J.J., 2018. Emission characteristics of $PM_{2.5}$ and trace gases from household wood burning in Guanzhong Plain, northwest China. Aerosol Science and Engineering 3, 130–140.